RESEARCH ARTICLE

Interaction of pesticides with natural and synthetic solids. Evaluation in dynamic and equilibrium conditions

Julián Ortiz Otalvaro[1] · Maximiliano Brigante[1,2]

Abstract
Interactions between pesticides (paraquat, glyphosate, 2,4-D, atrazine, and metsulfuron methyl) and soil organic and inorganic components have been studied in batch experiments by performing adsorption, dissolution, and chemical and photochemical degradation under different conditions. The obtained results confirm that the affinity of a pesticide to the solid surface depends on the nature of both and shows that each reactant strongly affects the mobility of the other one, e.g., anionic pesticides promote the dissolution of the solid humic acid but if this last is retained into the inorganic matrix enhances the adsorption of a cationic pesticide. Adsorption also seems to protect the bonded specie to be chemical degraded, such as shown in two pesticide/clay systems at constant pH. The use of mesoporous silicas could result in a good alternative for pesticide remediation. In fact, the solid shows high adsorption capacity towards paraquat and its modification with TiO_2 nanoparticles increases not only the pesticide adsorption but also seems to catalyze its degradation under UV light to less-toxic metabolites. UV-VIS spectroscopy was relevant and novel in such sense. Electrostatic interactions, hydrogen and coordinative bonds formations, surface complexations and hydrophobic associations play a key role in the fate of mentioned pesticides on soil and ground/surface water environments.

Keywords Pesticide removal · Soil components · Mesoporous silica · Solid-water interface · Interaction mechanisms · Pollution control

Introduction

Pesticides are, by definition, a group of chemical substances intended for preventing, destroying, repelling, or mitigating any pest. They can be classified according to their target, chemistry, or mode or period of action. Historically, inorganic products such as arsenic, copper, lead, and tin salts were used

as pesticides. However, they were prohibited or gradually fallen out in some countries due to their persistence in soil and their concern about the toxicity and contamination in groundwater. Modern pesticides are organic and often synthetic mimics of natural pest hormones which interfere with the growth of the target (bacteria, fungi, weeds, insects, nematodes, slugs, rodents, etc.) (Arias-Estévez et al. 2008).

Since the apparition of chemicals such as 2,4-dichlorophenoxyacetic acid and dichlorodiphenyltrichloroethane in 1930 and 1940, respectively, the amount of pesticides used in worldwide agricultural practices continuously increases and its production has been neither stopped nor decreased. For example, approximately 230,000 mt of herbicides have been used each year in the USA—since 2008—to control weeds in both agricultural and residential areas (USDA 2014). This represents an increase of 250% if it is compared with the amount applied in 1960. In Argentina, the world's third largest soybean producer, 960,000 mt of herbicides (83% ascribed only to glyphosate) were reported to be used in 2013. Recently, the Argentine Chamber of Agrochemicals (CASAFE 2012)

✉ Maximiliano Brigante
   brigante@uns.edu.ar

[1] INQUISUR, Departamento de Química, Universidad Nacional del Sur (UNS)-CONICET, Av. Alem 1253, B8000CPB Bahía Blanca, Argentina

[2] Consejo Nacional de Investigaciones Científicas y Técnicas (CONICET), Godoy Cruz 2290, C1425FQB Ciudad Autónoma de Buenos Aires, Argentina

issued a report on the evolution of Argentinean market: the use of pesticides increased 858% in the last 22 years, the cultivated areas increased 50%, but the crop yield only increased 30%. It is important to remark that the benefits that pesticides have played in increasing crop production at a reasonable cost are unquestioned. However, only a fraction (less than 1%) of the pesticides applied to crops actually reaches the target; the rest enters the environment gratuitously, contaminating soil, water, and air. Moreover, with an increase in the amounts used, concern about their adverse effects on non-target organisms, including animals and human beings, has also grown (Kaur et al. 2017; Pimentel and Levitan 1986). For example, the increasing use of pesticides is one of the factors attributed to the recently reduction—up to 50%—of the bee colonies in the USA. Fortunately, the society is aware of pollution with pesticides according to numerous reports in high-impact scientific journals (Eisenstein 2015; Fenner et al. 2013) and several articles appeared in recognized newspapers (Le Monde—France, May 2009; El País—Spain, February 2014; Clarin—Argentina, June 2014; The New York Times—USA, March 2015; The Daily Express—England, April 2016; Washington Post—USA, September 2016, etc.).

As soon as a pesticide is applied to its target, a number of natural processes immediately start to operate in order to remove the compound from the original site of application such as wash-off, run-off, volatilization, absorption, leaching, adsorption-desorption, dissolution-aggregation, and biological and (photo)chemical degradation (Arias-Estévez et al. 2008). There are so many (and complex) mechanisms that the models based on pesticide fate and transport hydrology used by the government regulatory agencies in many countries of North America and Europe are unrealistic and frequently fail (Gamble and Bruccoleri 2016). However, there is a consensus that those processes that involve the natural uptake of pesticides by soils and sediments are considered as the main cause of pollutant removal. Soil and sediments are constituted by both inorganic (clays, metal oxides, silicates, etc.) and organic (humic substances, polysaccharides, lipids, etc.) components. In fact, the major fractions of the refractory organic such as fulvic and humic acids can be found in the solid phase forming particles or solid aggregates, adsorbed at the surface of inorganic minerals or dissolved in the aqueous phase (Oste et al. 2002). Unfortunately, the dynamics of a pesticide to be removed depend not only on the nature of the pesticide (chemical structure, solubility, stability, etc.) and the soil (texture, permeability, pH, clay and organic matter content, slope, etc.) but also on climate factors and soil management. This leads to that a fraction of the mentioned soil constituents being good sorbents (or catalysts) in certain experimental conditions but with little or no capacity to remove the pesticide in natural conditions (Hseu et al. 2003) which facilitates its leaching into

groundwater. On the contrary, another fraction may have a high affinity for the pesticide protecting them in the adsorbed state from the attack of microorganisms and preventing its degradation (Scrano et al. 2005).

In order to progressively solve these problems, charcoal-derived materials, such as activated carbon and biochar, were applied as soil amendments. However, the solids fail in many aspects, e.g., they are inactive to remove hydrophilic and/or electrical-charged molecules; the presence of dissolved organic matter notably reduces their working capacity; they have short service life due to a poor and questionable regeneration; and the adsorption of organic chemicals with high molecular sizes is greatly impeded, or at least reduced, due to their microporosity (by size exclusion effect) (Liu et al. 2006; Vieno et al. 2007). For these reasons, researchers have focused their attention on the synthesis of solids with high surface area, meso- or macropores, and easy functionalization. Silica-based mesoporous materials fulfill with the mentioned purposes. These materials have several advantages in comparison with soils and soil components such as high surface area (> 200 m^2 g^{-1}), ordered pore distribution, narrow pore size distribution ($2 - > 10$ nm), high thermal stability, and easy regeneration and reusability (AlOthaman and Apblett 2010). Besides, its structure can be modified with organic (amines, thiols, alcohols, etc.) and inorganic (metal and metal oxide nanoparticles) species that enhances its removal properties (Brigante and Schulz 2011). For example, it is known that self-assembled monolayers on mesoporous silicas or SAMMS were recently used in the remediation of groundwater and sediments contaminated with heavy metals and radionuclides (Fryxell et al. 2007).

The aim of this article is to present a study of interaction between several pesticides and natural and synthetic adsorbents. Dissolution, adsorption, and degradation experiments were performed for such purposes. The data obtained at a variety of initial pesticide concentration, pH, ionic strength, temperature, etc. are used to gain insights into the mechanisms that govern the mentioned processes and into the factors that promote or prevent the removal of pesticides from aqueous and soil environments. The obtained results will also strengthen those reported by our research group in the past.

Materials and methods

Chemicals

Sodium chloride, potassium chloride, potassium hydroxide, and hydrochloric acid were obtained from Anedra. Tetraethyl orthosilicate (TEOS) and the surfactants cetyltrimethylammonium tosylate (CTAT), cetyltrimethylammonium bromide (CTAB), and Pluronic F68 were purchased from Sigma-Aldrich. Isonicotinic acid

($C_6H_5NO_2$, MW = 123.11 $gmol^{-1}$) was obtained from ICN Biomedicals Inc.

All investigated pesticides were chosen based upon their high application rate in Argentine agriculture. Paraquat dichloride (PQ^{2+}, MW = 257.16 $gmol^{-1}$), 2,4-dichlorophenoxyacetic acid (2,4-D, MW = 221.04 $gmol^{-1}$), glyphosate (GLY, MW = 169.01 $gmol^{-1}$), metsulfuron methyl (MSM, MW = 381.36 $gmol^{-1}$), and atrazine (ATZ, MW 215.68 $gmol^{-1}$) were obtained from Sigma-Aldrich. Molecular structures of studied pesticides and their acid dissociation constants and n-octanol/water partition coefficients are shown in the Supplementary Material (see Online Resource 1). PQ^{2+} is a dicationic pesticide whereas 2,4-D is anionic in aqueous solution and, thus, during all the experiments performed. This is due to the deprotonation of the carboxylic group of 2,4-D. GLY is also anionic in nature, with charges − 1, − 2, or − 3 depending on the solution pH due to the respective deprotonation of carboxylic, phosphonic, and/or amino groups in the molecule. Only at acidic media (around pH 2.3) GLY can be present as zwitterion. MSM is a weak acid whose protonated molecule is uncharged and predominates at pH < 3.3; the deprotonation of the nitrogen atom of the -SO_2NHCO- group results in an anionic specie that predominates at pH > 3.3. Finally, ATZ is found as an uncharged molecule in the environment.

All chemicals were of analytical grade and used as received. Doubly distilled water was used for the preparation of solutions.

Adsorbents

Goethite (GOET) and Na-montmorillonite (Na-MNT) were used as representative of soil inorganic matter whereas a humic acid (HA) was used as representative of soil organic matter. All solids were chosen because they are model sorbents for inactivating contaminants. GOET is an iron oxyhydroxide (α-FeOOH) and was prepared using a procedure similar to the described by Puccia et al. (2009). The formed solid is constituted by well-crystallized acicular particles whose surface area and point of zero charge/isoelectric point are 57.6 $m^2 g^{-1}$ and 8.9, respectively. The montmorillonite used in this study, whose chemical formula is ($Al_{2.78}Fe_{0.40}Mn_{0.18}Mg_{0.64}$)$^{IV}O_{20}(OH)_4$ (M is the monovalent exchangeable cation), was obtained from a deposit in Cerro Banderita (Neuquén, Argentina). The < 2 μm solid particles were treated with a 1 M NaCl solution in order to obtain the Na-MNT. The solid has a cation exchange capacity (CEC) of 91.7 mEq·100 g^{-1}; total and external surface areas of 974.7 and 6.7 $m^2 g^{-1}$, respectively; and a basal spacing of 12.6 Å.

In order to evaluate the importance of organic matter in the soil matrix, a composite formed by GOET and HA (HA-GOET) was synthesized. The synthesis was performed by treating 50 mL of a 23.17 g L^{-1} goethite dispersion (pH 8.7 in 0.1 M KCl) with 450 mL of a 200 mg L^{-1} HA solution (pH 8.7 in 0.1 M KCl). The HA sample used in this work was taken from an andisol (Boqueixon, A Coruña, Spain) and purified according to the International Humic Substance Society procedures. The solid HA was formed by amorphous particles of different shapes and sizes, whose average size is 250 μm. The elemental composition of the sample is N (4.86%), C (52.57%), H (5.06%), O (34.77%), and S (0.33%), and contained some Fe (1.65%) and Al (0.76%) impurities. Solid state ^{13}C nuclear magnetic resonance indicated that the studied sample contains 29% of alkyl C, 38% of O-alkyl C, 19% of aromatic and phenolic C, 11% of carboxyl C, and 3% of carbonyl C. The content of HA on the composite is 4.88% and its surface area is 38.7 $m^2 g^{-1}$.

As non-natural adsorbents were used a mesoporous silica (SiO_2) with hexagonally pore arrays, like as MCM-41, and the same material modified with TiO_2 nanoparticles in order to evaluate the inclusion of a metal oxide on the adsorbent and photocatalytic properties of silica. SiO_2 was synthesized in alkaline media by using TEOS as a silica precursor and a mixture of the surfactants CTAT and Pluronic F68 as a pore structure directing agent. The synthesized solid, named SiO_2-A, consists of agglomerates of polydisperse plate-like particles of around 1.5 μm and whose surface area, pore diameter, and isoelectric point are 468 $m^2 g^{-1}$, 2.84 nm, and 2.2, respectively. For comparative purposes, CTAB was also employed as template. The formed material, called SiO_2-B, has a surface area, pore diameter, and isoelectric point of 238.6 $m^2 g^{-1}$, 18.9 nm, and 3.5, respectively. TiO_2-SiO_2 was synthetized in a similar way as the SiO_2-B procedure where a known amount of titania nanoparticles were suspended in the CTAB solution before interacting with TEOS and the alkali solution. TiO_2 nanoparticles (98% anatase phase, average size of 6 nm) were previously obtained by using an inverse microemulsion composed by n-hexane/water/Aerosol OT (Brigante and Schulz 2011). The surface area and isoelectric point of the synthesized TiO_2 and TiO_2-SiO_2-B are 9.5 and 259.2 $m^2 g^{-1}$ and 6.7 and 4.2, respectively.

More details about the synthesis procedure and characterization of all used solids can be found elsewhere (Brigante and Schulz 2011; Brigante et al. 2008, 2013; Puccia et al. 2009).

Pesticide-solid interaction experiments

HA dissolution

Dissolution experiments of the HA sample were carried out in a cylindrical, temperature-controlled reaction vessel covered with a glass cap. After adding 50 mL of a 10^{-3} M KCl solution (control) to the reaction vessel, with or without the addition of a desired amount of the pesticide, and setting the temperature and pH at the desired value, a charge of 8–10 mg of HA was

approximately added to the reactor while stirring the content of the reactor at 450 rpm. During all the experiment, the suspension was purged with N_2, and the pH was adjusted with KOH and/or HCl solutions. After 6 h of reaction, required time to reach complete dissolution or to gather enough data points (Brigante et al. 2008), the particles were separated from the supernatant by centrifugation and it was immediately analyzed by UV-VIS spectroscopy at 400 nm to quantify the concentration of dissolved HA. The pH was checked periodically and kept constant by adding minute volumes of concentrated KOH or HCl solutions when necessary. Calibration curves at the working pH were constructed with several HA solutions having concentrations that ranged between 2 and 200 mg L^{-1}. A uniform absorption coefficient was assumed for the different dissolved fractions, which gives rather accurate concentration values (Brigante et al. 2008). HA dissolution behavior was tested under reaction conditions which were as follows: temperature at 25 °C, initial concentration of pesticides from 0 to 3×10^{-3} M, and pH from 4 to 11. Some experiments were carried out per triplicate in order to evaluate the reproducibility of the dissolution process.

The percentage of dissolved HA, DHA(%), was evaluated as follows:

$$\mathrm{DHA}(\%) = \frac{C_{\mathrm{HA}}}{C_T} \times 100, \tag{1}$$

where C_{HA} is the HA concentration in the supernatant and C_T is the total concentration of HA that would be present in the supernatant after complete dissolution of the solid. The magnitude of C_T was calculated from the initial weight of HA and the volume of KCl solution used in the dissolution run.

Adsorption

Batch adsorption experiments on studied materials were performed in 15 mL polycarbonate centrifuge where 50 mg of adsorbent, proper volumes of KCl solution (used as supporting electrolyte), and appropriate aliquots of pesticide were introduce into the tubes. The final volume was 10 mL and the range of initial pesticide concentration was situated between 10^{-6} and 10^{-3} M. Small amounts of either KOH or HCl solutions were added to achieve the desired pH in all experiments. The tubes were shaken end-to-end during 6 h to ensure equilibration and the pH was checked and kept constant periodically. The tubes were then centrifuged at 4500 rpm for 10 min and the supernatants were withdrawn and analyzed by UV-VIS spectroscopy (Agilent 8453 UV-VIS diode array spectrophotometer) to quantify the concentration of adsorbed pesticide. In GOET, HA-GOET, and Na-MNT systems, the centrifuged supernatants were also filtered using 0.2-μm pore-diameter cellulose acetate filters

(Osmonic) prior to analysis. The adsorbed pesticide was calculated from the difference between the initial adsorbate concentration and the concentration of the species that remained in the supernatant solution. Pesticide adsorption behavior was tested under reaction conditions which were as follows: pH from 4.5 to 9.5, temperature from 5 to 45 °C and KCl concentration from 0 to 0.3 M. Some experiments were carried out per duplicate in order to evaluate the reproducibility of the adsorption process.

The adsorption isotherms were fitted using a Langmuir equation, which was commonly used in the adsorption of pesticides on several adsorbent systems (Tsai et al. 2005). The linear form of this equation is displayed as follows:

$$\frac{1}{q_{\mathrm{ads}}} = \frac{1}{q_{\mathrm{mon}}} + \frac{1}{q_{\mathrm{mon}}K_L C_{\mathrm{eq}}}, \tag{2}$$

where q_{ads} is the adsorbed amount of adsorbate (μmol g^{-1}), C_{eq} is the equilibrium concentration of pesticide in the supernatant (μmol L^{-1}), q_{mon} is the maximum amount of molecule adsorbed (μmol g^{-1}) corresponding to complete coverage on the surface, and K_L is the Langmuir constant (L μmol^{-1}). From the linearized form of Eq. (2), q_{mon}, K_L, and the correlation coefficient, r^2, can be calculated.

Chemical degradation

Degradation kinetics of PQ^{2+} and MSM in aqueous solution was performed in batch experiments, using 50 mL polypropylene centrifuge tubes covered with polypropylene caps. Twenty milliliters of a 175 μM stock PQ^{2+} solution (or a 38.3 μM stock MSM solution) and known amounts of Na-MNT were introduced in each centrifuge tube and mixed with a KCl solution, which was used as supporting electrolyte. The total volume was 35 mL and the resulting concentrations of KCl and PQ^{2+} (or MSM) were 0.01 M and 100 μM (or 21.9 μM), respectively. The pH of the solutions was then adjusted to the working pH by adding HCl or KOH. The tubes were shaken with an end-over-end rotator (FAES, Argentina) and the pH was checked and kept constant periodically. At different reaction times, an aliquot of the solution was withdrawn and its UV-VIS spectrum was obtained. After registration of the spectrum, that took around 30 s, the solution was reintroduced into the tube. This procedure was repeated during several hours or even days in order to achieve a complete degradation of the pesticide or to gather enough data points. Pesticide degradation behavior was tested under reaction conditions which were as follows: pH from 3 to 10.5, temperature at 25 °C and initial Na-MNT concentration from 0 to 8.1 g L^{-1}. The pH

values were chosen due to the stability of these pesticides in aqueous solution at neutral pH (Brigante et al. 2009).

The kinetics can be evaluated by plotting the percentage of degraded pesticide, $DP(\%)$, as a function of the reaction time, t. $DP(\%)$ was calculated as

$$DP(\%) = \left[1 - \left(\frac{A - A_f}{A_i - A_f}\right)\right] \times 100, \qquad (3)$$

where A is the absorbance at time t, A_i is the initial absorbance at the working wavelength, and A_f is the final absorbance, which corresponds to complete degradation. Complete degradation of MSM was observed in experiments at extreme pH values (2 and 11.5) (Brigante et al. 2013); thus, A_f is obtained by degrading completely MSM at either pH 2 or 11.5 and then changing the pH of the resulting solution to the pH value at which the degradation was studied. If the pesticide is stable for degradation, A_f is avoided. The working wavelength was 257 nm at all studied pH for the case of PQ^{2+} whereas 233 and 245 nm were for the case of MM at pH 3 and 10.5, respectively, due to the shifting of its maximum absorption band as pH varies.

Photochemical degradation

TiO$_2$ nanoparticles are known to be a very good photocatalyst of several pollutant species in water such as dyes, antibiotics, and pesticides (Brigante et al. 2011; Gautam et al. 2016) because it stimulates the formation of hydroxyl and oxygen radicals for oxidizing the target molecule. Its catalytic activity strongly increases if the particles are disperse over a support. In such sense, 200 mg of TiO$_2$-SiO$_2$-B were added into 100 mL of a 150 μM PQ^{2+} solution in a cylindrical, water-jacketed reaction vessel. The reaction temperature was maintained constant at 25 ± 0.2 °C and the pH of the suspension was adjusted at pH 9.5 with KOH and/or HCl solutions. The reactor was placed at a fixed distance of 20 cm from a DESAGA UV 131000 lamp ($\lambda = 366$ nm) and was stirred at a constant speed throughout the photoreaction process. Light intensity was estimated as $I_a = 2.7 \times 10^{-6}$ molphotons^{-1}. At different reaction times, a 5-mL aliquot was withdrawn, the particles were separated from the supernatant by centrifugation at 5000 rpm, and the supernatant was immediately analyzed to quantify the concentration of degraded PQ^{2+} by UV-VIS spectroscopy at 257 nm. After the quantification, that took around 30 s, the supernatant and the catalyst particles were reintroduced into the reaction vessel. This procedure (aliquot withdrawal, separation, quantification of PQ^{2+}, and reintroduction of the aliquot into the reaction vessel) was repeated during several hours or even days in order to achieve complete degradation of the pesticide or to gather enough data points. The pH was checked periodically and kept constant by adding minute volumes of concentrated KOH or HCl

solutions when necessary. To discriminate between both effects, i.e., adsorption and photodegradation, a similar experiment was performed in the darkness and the results were subtracted from those carried out under irradiation. The photodegradation kinetics can be also evaluated by plotting Eq. (3) as a function of t.

Results and discussion

HA dissolution

The reactivity of a HA particle, i.e., its tendency to dissolve, depends on the type, number, and strength of the forces that keep together HA molecules in the solid phase, and on the ability of dissolved ions or molecules to weaken or strengthen those forces. This phenomenon is also influenced by other variables such as climatic (e.g., temperature) and water volume and flow conditions (Brigante et al. 2007). Figure 1 shows the effect of the concentration of several pesticides on the percentage of dissolved HA at pH 7. Neutral pH was chosen for this experiment because this is a desirable soil pH value for crop production due to the availability of most nutrients to plants (Séquaris et al. 2013). It can be seen in the figure that pesticides with a negative charge development in aqueous solution strongly increase the dissolution of HA whereas PQ^{2+}, a divalent cation, decreases it as the pesticide concentration increases. It is also interesting to note that GLY increases DHA(%) up to almost four times in comparison with the experiments performed in a 10^{-3} M KCl solution (control) but never reaches complete dissolution. It is due to the fact that the rupture of H-bonds that contribute to hold HA molecules together in the solid and the electrostatic repulsion among negative-charged humic molecules also depends on the solution pH (Brigante et al. 2007; Milne et al. 2001). Similar
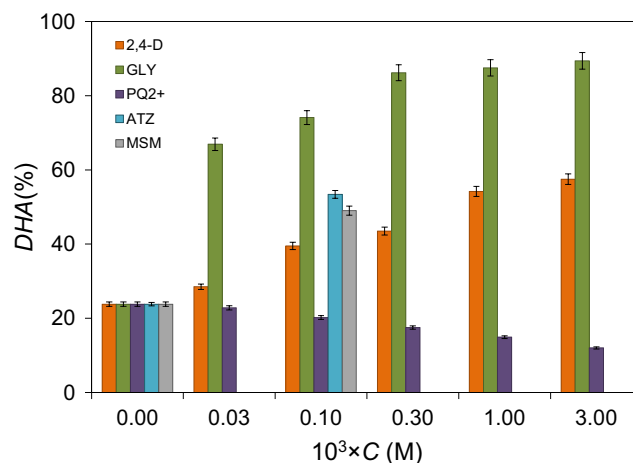

Fig. 1 Effect of concentration of several pesticides on the percentage of dissolved HA at pH 7 and 25 °C. Error bars represent the standard deviation of experiment replicates

results are found in the presence of other anionic pesticides such as 2,4-D and MSM, or in the presence of the neutral ATZ. The increase of DHA(%) by non-cationic pesticides is attributed to an adsorption process on the surface of HA particle. This attachment leads to the formation of surface species that weaken the interactions between HA molecules at the surface of the particles leaving them susceptible for detachment. GLY and 2,4-D are known to form H-bonds with the oxygen groups of HA (Barja et al. 2001; Larrivee et al. 2003). Dutta et al. (2015) showed that MSM and ATZ also form H-bond with the polar group of HA molecules, although the authors suggested that non-specific interactions (hydrophobic interactions with aromatic and/or aliphatic HA domains) should not be discarded in ATZ mainly because it is less hydrophilic than MSM, i.e., log Kow = 2.61 for the case of ATZ in comparison with log Kow = 0.018 for the case of MSM. Besides H-bonds and hydrophobic forces, our research group suggested that GLY and 2,4-D may also coordinate metal ions such as Fe(III) and Al(III) which are impurities of the HA sample (Brigante et al. 2009). ATZ and MSM seem to form complexes with transition metal ions too, taking into account the results reported by Kumar et al. (2015) and Pei et al. (2008). This kind of complexation could also take place at the surface of the studied HA and thus dissolution could be also promoted by the presence of the mentioned pesticides. PQ^{2+}, on the contrary, decreases two times DHA(%) as the pesticide concentration increases preventing thus the passage of HA molecules to the bulk solution. This effect is stronger at higher pH, such as shown in Online Resource 2. The decrease in DHA(%) can be also explained by an attachment of the pesticide to the surface of HA particle. However, it may be speculated that adsorbed cations can (i) decrease the net negative charge of HA molecules decreasing the electrostatic repulsion between them and (ii) act as bridges between functional groups of two adjacent molecules at the surface increasing the attractive forces between them (Brigante et al. 2007). Both effects will end up with a decrease in dissolution. Finally, it can be seen in the figure that the dissolution behavior is highly reproducible with an error ranged between 1.5 and 2.5% depending on the pesticide-HA system.

In a previous paper (Brigante et al. 2009), we reported the possible two-step dissolution mechanism of HA particles from kinetics experiments. In the case of dissolution of solid HA promoted by anionic pesticides, the fast step is ascribed to the adsorption of these molecules to the surface of HA particles forming surface species. Such species are then responsible for weakening the interactions between HA molecules at the surface of the particles, such as hydrogen bonds, p-bonds, coordinative bonds with metal impurities, van der Waals forces, and hydrophobic interactions. The second and rate-determining step is attributed to the release of these surface molecules to the solution bulk. In the case of dissolution affected by cationic pesticides, on the contrary, the fast

adsorption diminishes the electrostatic repulsion among the molecules, which ends up with a decreased dissolution rate.

Figure 2 shows the effect of pesticides on the percentage of dissolved HA at several pH values. In the absence of herbicides, the effects of pH were already discussed in a previous publication (Brigante et al. 2007) and were attributed to the progressive detachment of the proton from carboxylic and phenolic groups of HA molecules as the pH increases. This causes the breaking of hydrogen bonds that hold HA molecules in the solid phase, the increasing of the electrostatic repulsion among negatively charged molecules and therefore, the rising of DHA(%). As expected, GLY and 2,4-D enlarge the percentage at almost all investigated pH, except at pH > 9 where dissolution is similar to the control. This weak effect is attributed to the electrostatic repulsion between the functional groups of pesticides (carboxylate for the case of 2,4-D and mainly phosphonate for the case of GLY) and the negative-charged HA molecules which impede their adsorption. However, PQ^{2+} decreases DHA(%) at high pH but increases it at pH < 6. The obtained results suggest that the pesticide interact with the solid HA molecules by different kinds of interactions which are pH dependent. The effects at pH > 6 can be well understood assuming that PQ^{2+} is blocking part of the negative-charged surface upon adsorption. The effects at low pH seem to be attributed to non-electrostatic interactions such as hydrophobic associations. In such sense, Rodríguez-Cruz et al. (2009) showed that the adsorption of PQ^{2+} on commercial lignins (lignin is one of the HA constituents) can be explained in terms of the variability of the polarity index and the octanol–water partition coefficient of sorbent and sorbate. In an earlier paper (Brigante et al. 2008), we showed a linear relationship between the dissolution rate of HA and the length of hydrocarbon chain of monocarboxilic acids, i.e., the larger the number of carbon atoms in the acid,
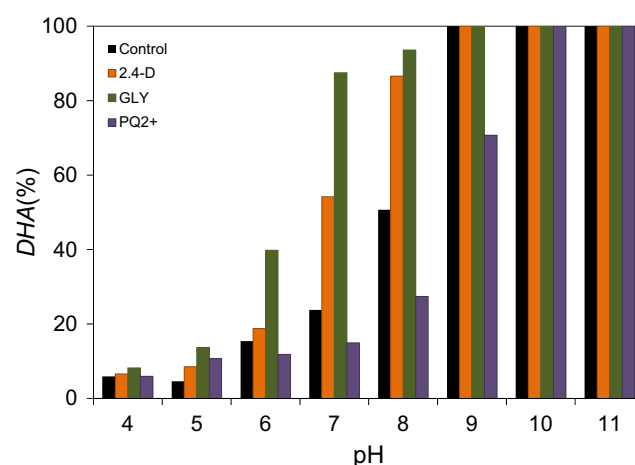
Fig. 2 Effect of pH on the percentage of dissolved HA in presence of a 10^{-3} M pesticide solution at 25 °C. Control is called to the experiments performed in a 10^{-3} M KCl solution at the working pH in the absence of pesticides

the greater the affinity for the hydrophobic components of HA, and the greater their capacity to alter the humic associations. On basis of the mentioned results, it is feasible that PQ^{2+} can weaken or disrupt attractive forces among humic molecules by hydrophobic associations increasing the capacity of HA dissolution at acidic pH.

Adsorption

In view of the results showed above, the dissolution of solid HA aggregates makes this material a poor system to deactivate the mobility of several pesticides through the aqueous sources. Only cationic species (metal ions, soil components with positive charge development, etc.) or acidic water environments seem to reduce this phenomenon. Therefore, other solids must be studied as adsorbent of pesticides in order to reduce (i) its transport across the surface waters or (ii) its leaching into groundwater. Figure 3 shows the adsorption of PQ^{2+} (represented by the q_{mon} value) on both natural soil components and synthetic adsorbents at several pH values.

The adsorption of PQ^{2+} on GOET and TiO_2 is negligible. At pH values lower or near the isoelectric point, the GOET surface has a net positive charge and electrostatics restricts the adsorption of the dication. In addition, PQ^{2+} does not have the ability of transition metal cations to form inner-sphere surface complexes with surface sites of the solid and overcome electrostatics, as seen by Saito et al. (2004) for the adsorption of Cu^{2+} on GOET. Although TiO_2 has a lower isoelectric point than GOET, the absence of adsorption is mainly ascribed to its low surface area.

On the contrary, the adsorption of PQ^{2+} on the other studied solids is high, significant, and reproducible. The shape of the isotherms (data shown in Online Resource 3) is similar to those reported in literature for the adsorption of this kind of pesticide (Brigante and Avena 2014; Tsai et al. 2005). The adsorption is very fast (50 min or lower is necessary to reach

the adsorption equilibrium) and it is strongly dependent on the pH, i.e., it is high at pH 9.5 and it decreases significantly at pH 7 and 4. The dependence on the pH is attributed to an increase of surface negatively charged sites of the adsorbents that are available for the cationic pesticide due to the loss of H^+ from the surface and, thus, increasing the electrostatic attractions between them as pH increases. In Na-MNT, q_{mon} does not vary significantly with the pH because the surface charge of basal faces (representing 98% of the total surface area) is not pH dependent (Draoui et al. 1999). The maximum adsorption of around 457 $\mu mol\ g^{-1}$ is closed to the CEC of the clay in agreement to those reported by Rytwo et al. (1996) for cation exchange process of this pesticide in similar conditions with other divalent organic cations (diquat, crystal violet, and acriflavine) on montmorillonite. Interaction between PQ^{2+} and the adsorbents can be visualized comparing the FTIR spectra before and after adsorption occurs, such as shown in Online Resource 4. Apparition of new peaks located at 1647, 1458, and 830 cm^{-1}, which are assigned to the C–C tension mode and the C–H deformation mode in the aromatic ring plane of PQ^{2+}, confirms the binding between the herbicide and the solids.

It is also interesting to note that the adsorption of PQ^{2+} on the composite is much higher than in the bare solid. The adsorption capacity in HA-GOET is higher than in the bare iron oxide because the humic molecules generate more negative sites for the pesticide being adsorbed (Iglesias et al. 2010). The high adsorption capacity in TiO_2-SiO_2-B in comparison with SiO_2-B is attributed to the fact that the dispersion of the titania nanoparticles over the silica support offers more active sites for adsorption than non-supported TiO_2 due to the agglomeration of particles (Phanikrishna Sharma et al. 2010). Figure 3 also shows that the experimental conditions in which the adsorbent was synthesized play a key role too. In effect, the adsorption on SiO_2-A is 25 times higher than on SiO_2-B, i.e., in this last, the adsorption is only detectable at pH 9.5. This is attributed to the differences in surface area and porosity of the studied materials.

Regeneration and reuse of the adsorbent is a crucial point to be evaluated from the technology point of view; the commonly used methods are solvent extraction or air-flux calcination. However, none of the methods can be applied to the natural soil constituents. On the one hand, calcination causes phase changes in the solid matrix or generates CO_2 and other greenhouse gases if organic compounds (with C, N, and S atoms) are adsorbed on their surfaces (Chen et al. 2010; Tanev and Pinnavaia 1995). On the other hand, solvent extraction cause dissolution of soil constituents, i.e., iron oxides and motmorillonites are known to be (total or partial) dissolved by acidic solvents and HA is able to be dissolved or desorbed from the support surface by alkaline solvents (Rozalen et al. 2009; Sidhu et al. 1981). Moreover, Ramos et al. (2014) reported that oxides and clay can be dissolved at neutral pH by
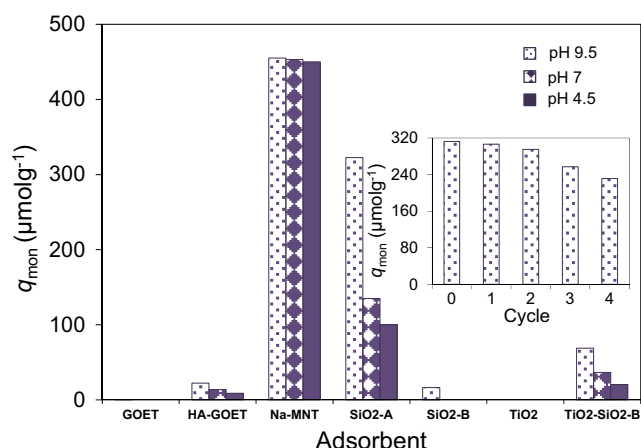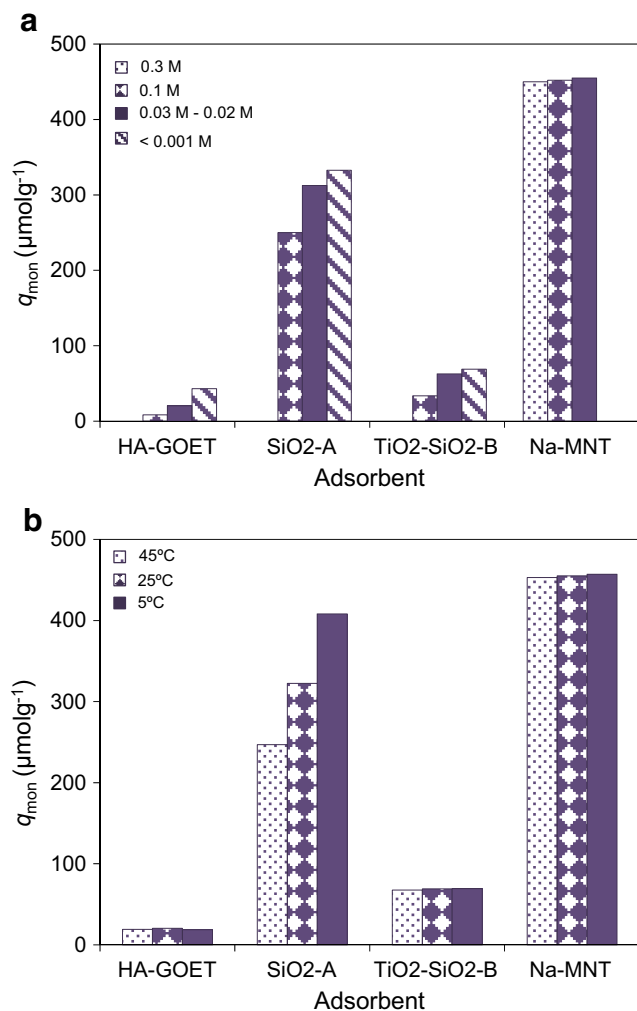

Fig. 3 Effect of pH on the adsorption of PQ^{2+} on the studied adsorbents at 25 °C. The inset shows the PQ^{2+} adsorption capacity of SiO_2-A after several regeneration and reuse cycles at pH 9.5

complexing agents such as oxalate ions. Due to its chemical and thermal stability, mesoporous-based silica materials are available to be used in such experiments. As shown in the inset of Fig. 3, SiO_2 can be reused in almost 4-times adsorption-desorption cycles with very good effectivity and without altering the silica structure after three times regeneration by HCl-water extraction treatment. Similar results were recently obtained by Rivoira et al. (2016) on the adsorption of GLY on $Fe-NH_2-SiO_2$.

Figure 4 shows the effect of ionic strength and temperature on the adsorption of PQ^{2+} on several adsorbents at pH 9.5. This pH (and not pH 7) was chosen due to the major capacity of the pesticide to be adsorbed by the studied solids. Except for Na-MNT and its charge development, the adsorption is strongly dependent on the ionic strength, decreasing as KCl concentration increases such as shown in Fig. 4a. The negative dependence of the adsorption of PQ^{2+} with the ionic strength is consistent with formation of outer-sphere complexes or ionic pairs, where there is competition with the cations of the supporting electrolyte. Similar results were reported by Nakamura et al. (1999) on the adsorption of PQ^{2+} on activated carbon. The electrostatic attractions between adsorbate and adsorbent are also evidenced by varying the adsorption temperature. While the affinity of PQ^{2+} on SiO_2-A strongly decreases as temperature increases the process seems to be not affected, or slightly influenced, by the temperature in the other solids, such as shown in Fig. 4b. The no dependence of the adsorption with the temperature is also consistent with formation of ionic pairs or outer-sphere complexes, where there is competition with the cations of the supporting electrolyte. If changes in temperature affect in a similar way the affinity of PQ^{2+} and K^+ for negatively charged sites, there will be no significant temperature effects by changing the temperature. From adsorption data at several temperatures, the thermodynamic parameters Gibbs free energy ($\Delta G°$), enthalpy ($\Delta H°$), and entropy ($\Delta S°$) for the adsorption of PQ^{2+} on the studied materials can be also obtained. The calculated parameters are shown in Online Resource 5 and indicate that the adsorption in all solids is spontaneous in nature.

The adsorption of the other pesticides employed in the "HA dissolution" section strongly depends on its chemical nature. For example, the adsorption of MSM on GOET and Na-MNT is low and only detectable at pH 4 or lower with a q_{mon} value of around 5–6 $\mu mol\ g^{-1}$, and it is negligible on both bare and modified SiO_2. H-bond formations between the functional group of the mentioned soil constituents and the pesticide—with a high percentage in the protonated form according to its acid-base equilibrium—seem to play a key role on the adsorption. The middle-low affinity to solids is also detected in 2,4-D, i.e., a q_{mon} of 20 $\mu mol\ g^{-1}$ is calculated from the adsorption experiments on GOET at pH 3 and then it decreases to almost zero at pH 4.5 (data not shown) whereas the adsorption of the pesticide on Na-MNT was negligible in all studied pH. Electrostatic interactions between the negative-charged clay (or positive charge GOET) and the carboxylate functional group of 2,4-D explain the differences on the adsorption behavior (Clausen and Fabricius 2001). Electrostatic repulsions are also expected to take place in the negative-charged SiO_2 (Goyne et al. 2004). However, Hermosin and Cornejo (1992) reported that the modification of montmorillonites with cationic surfactants strongly adsorbs the pesticide through the formation of H-bonds between carbonyl group of 2,4-D and ammonium group of the interlayer organic cations. According to literature, C-rich materials such as graphene can be also used as a promising adsorbent for removing the pesticide due to its possibility to form π-π associations between the benzene ring of 2,4-D and the solid (Liu et al. 2016). For the case of ATZ, no adsorption was detected on the studied materials attributed to the non-polarity of the pesticide (Clausen and Fabricius 2001). However, Bia et al. (2017) recently showed that the modification of a Na-MNT with humic acids and Fe(Hydr)oxide strongly enhances its adsorption capacity.


Fig. 4 Effect of **a** ionic strength and **b** temperature on the adsorption of PQ^{2+} on the studied adsorbents at pH 9.5

GLY is, on the contrary, a pesticide that strongly binds iron oxides and clay particles. Dos Santos Afonso and co-workers (Barja and Dos Santos Afonso 2005; Damonte et al. 2007) reported that the adsorption of GLY on GOET and Na-MNT is high, with q_{max} values (q_{max} is the maximum value of obtained q_{mon}) of around 144 and 283 μmol g^{-1}, respectively. The authors also indicated that the adsorption on both solids strongly depends on the pH and ionic strength, increasing as pH decreases and as ionic strength increases, related to the formation of inner-sphere complexes between phosphonate group of GLY and the functional group of the solids (e.g., iron surface hydroxyls or clay exchangeable ions). However, the presence of HA on the composite significantly affect the adsorption. In fact, Arroyave et al. (2016) showed that the adsorption of GLY strongly decreases as the amount of HA supported on GOET increases due to the electrostatic repulsion between the pesticide and HA.
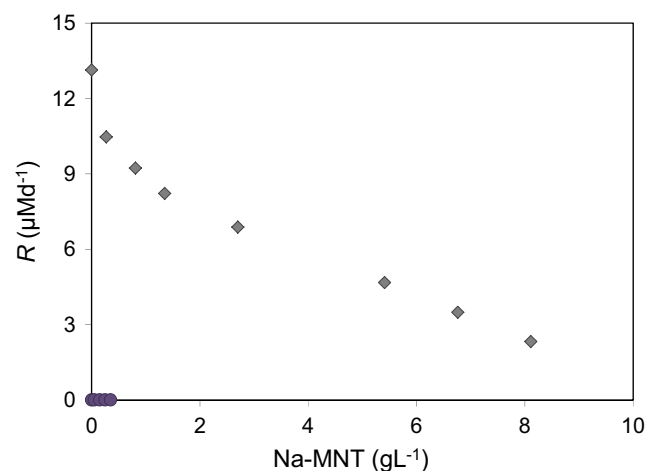
Chemical degradation

Figure 5 shows the effects of pH on the percentage of degraded MSM and PQ^{2+} in aqueous solution as a function of time. The kinetic strongly depends on the pH for the case of MSM. It is relatively fast at pH 3, where only 24 h were necessary to degrade 50% of the initial pesticide and around 8–10 days to achieve complete degradation. The reaction becomes significantly slower at pH 10.5 leading to a 65% degraded MSM after 30 days. The degradation mechanism is mainly ascribed to the cleavage of the sulfonylurea linkage via attack by water in acid media, or by the O-demethylation of the methoxy-triazine moiety followed by hydrolytic cleavage of the triazine ring at alkaline pH (Sarmah et al. 2000; Sarmah and Sabadie 2002). At near neutral pH range, the degradation was from very low at pH 6 with a half-life coefficient of around 1.5 years
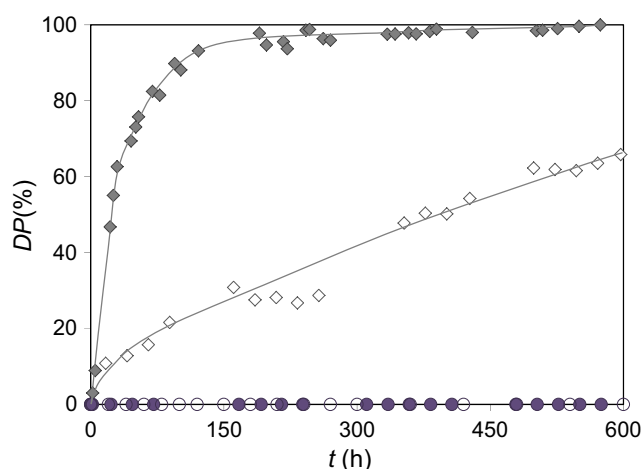
to negligible at pH 7 (Brigante et al. 2013). PQ^{2+}, on the contrary, is stable at all studied pH. In fact, the UV-VIS spectrum with a maximum absorbance at 257 nm did not change (neither in shape nor in intensity) with time during the month the experiments were carried out. Although the high chemical stability that the pesticide offers in aqueous solution is known, i.e., it has a half-life coefficient of around 23 weeks (USEPA 1987), Roberts et al. (2002) suggested that PQ^{2+} begins to hydrolyze at pH > 12. Microbial (Roberts et al. 2002) and catalysis assisted degradation (Diaz Kirmser et al. 2010; and see below) seem to be the main routes of PQ^{2+} metabolism.

Figure 6 shows the evolution of the degradation rate, R, as a function of the clay concentration. R is calculated from degradation curves, as shown in Fig. 6, assuming a first-order kinetic. Taking into account the results presented in the "Adsorption" section, the adsorption of PQ^{2+} on Na-MNT is almost 100 times higher than of MSM. The behavior is understandable since MSM exists predominantly as a neutral molecule at pH < 3.3 and thus interactions between MSM and the clay surface are not electrostatically driven. The binding is attributed to hydrogen-bond formations or other kinds of interactions, which are weaker than electrostatic attractions, leading to a lower adsorption than in the case of PQ^{2+} species. However, the adsorbed MSM seems stable to be degraded. In fact, the degradation rate decreases by increasing clay concentration. This protective action is mainly due to adsorption, i.e., adsorbed MSM molecules do not degrade whereas MSM molecules that remain in solution degrade (Brigante et al. 2013). Therefore, at low clay concentration, MSM concentration in the supernatant is high and the degradation rate is relatively high; at high clay concentration, the pesticide concentration is quite low due to a major adsorption and then the degradation rate is low. As expected, the high affinity of the clay by the cationic pesticide does not catalyze the degradation of neither the adsorbed nor the supernatant PQ^{2+}, i.e., the remaining solution is not degraded by Na-MNT at clay concentration

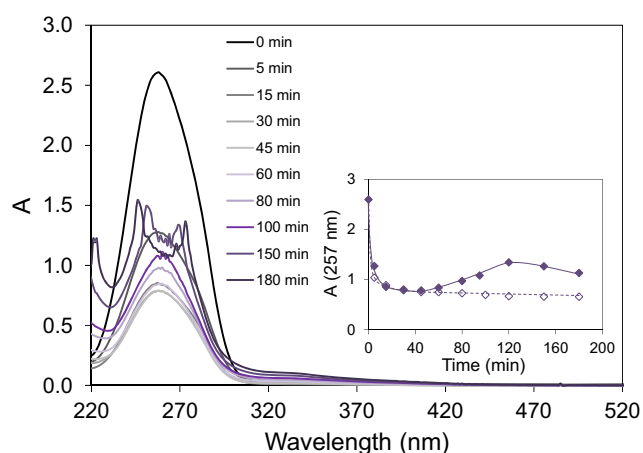Fig. 5 Effect of pH on the percentage of degradation of MSM (diamonds) and PQ^{2+} (circles) as a function of time. pH: solid symbols, pH 3; and open symbols, pH 10.5. Initial Na-MNT concentration: 2.7 g L^{-1} for MSM and 0.15 g L^{-1} for PQ^{2+}. Lines are used as a guide

Fig. 6 Effect of clay concentration on the degradation rate of MSM (diamonds) and PQ^{2+} (circles) at pH 3 and 25 °C

below 0.35 g L^{-1} whereas the initial pesticide concentration is completely adsorbed at 0.50 g L^{-1} or higher.

Photochemical degradation

Figure 7 shows the evolution of the UV-VIS spectra of a PQ^{2+} solution during a typical photodegradation kinetic experiment performed at pH 9.5. The maximum absorbance of PQ^{2+} (located at 257 nm) decreases continuously in time and eventually reaches a constant value after 45 min of reaction. This is attributed to the fast adsorption of PQ^{2+} on the solid surface (Brigante and Avena 2014). Similar experiments performed in darkness confirm that the adsorption equilibrium is being reached after 40 min of reaction. The spectrum suffers then several alterations (in intensity and shape) as the irradiation time increases indicating that degradation process is happening too although more slowly than the adsorption step.

As far as we know, changes in the UV-VIS spectrum of PQ^{2+} during their photodegradation kinetics were never reported. The increase of absorbance after 45 min of reaction is mainly attributed to the oxidation of the pesticide due to oxidizing radicals. In fact, the shape of spectrum at 100 min seems to indicate the formation of a derivate of nicotinic acid with maximum absorption peaks at around 212 and 260 nm (Trivedi et al. 2015) such as shown in Online Resource 6. The spectrum takes then several (and unknown) shapes with the apparition of a shoulder at around 340 nm whose intensity increases as irradiation time increases. This seems to suggest that other metabolites are also being formed, e.g., nitrate and nitrite ions with a maximum absorption at around 302 and 354 nm, respectively (Jankowski et al. 1999) could be responsible of the shoulder formation. The obtained results are different from those reported by Moctezuma et al. (1999). The

authors detected only the decrease in intensity of the 257 nm band with the time indicating that 100% of the pesticide is degraded after 120 h of reaction. Unfortunately, it is not possible to quantify the amount of degraded PQ^{2+} in our case, i.e., the maximum absorbance decreases during the first 40 min (mainly due to adsorption), and then it increases up to 120 min and finally decreases, such as shown in the inset of Fig. 7. More sophisticated detection methods, such as mass spectrometry, are needed to quantify the amount of degraded pesticide, i.e., monitoring the decay of PQ^{2+} signal at m/z 186 (Florêncio et al. 2004). Finally, it is also important to indicate that the degradation of PQ^{2+} in the absence of the catalyst was not detected in agreement with the results reported by Florêncio et al. (2004).

There are several studies about the mechanism of PQ^{2+} degradation. Roberts et al. (2002) reported a revision about the fate and metabolism of PQ^{2+} in soil environments. The pesticide is photodegraded firstly to form paraquat monopyridone and/or monoquat. Either metabolites are then degraded to 4-methyl isonicotinic acid (QINA) which would be in agreement with the observed spectrum at 100 min. QINA is finally degraded to methyl amine and CO_2. Other intermediates such as paraquat dipyridone, compounds with molecule formula $C_6O_5H_8$ and $C_7NO_3H_{10}$, ammonium ion, and nitrate/nitrite ions (this last in accordance with our results) are also reported using TiO_2-based catalysts (Nghia et al. 2017; Florêncio et al. 2004; Tennakone and Kottegoda 1996). Recently, Kreunetr and Wanchanthuek (2017) suggested that H_2O and CO_2 are the final metabolites on the degradation of PQ^{2+} under both solar and UV light irradiation using Fe/TiO_2 nanoparticles as catalyst. However, the authors could not propose a mechanism or identify intermediate products due to the technique implemented, i.e., voltammetry, did not permit to detect them.

According to the literature, TiO_2-SiO_2-based materials are also good catalysts in the degradation of ATZ and GLY reaching individually 83.4 and 100% of decomposition after UV irradiation during few hours (Li et al. 2013; Mangat Echavia et al. 2009). Cyanuric acid and nitrate, phosphate, and carbon dioxide were reported as the mainly photodegradation metabolites of ATZ and GLY, respectively.

Fig. 7 Evolution of the UV-VIS spectrum of PQ^{2+} supernatant before and after interaction with TiO_2-SiO_2-B under UV light irradiation at pH 9.5. The inset shows the variation of the maximum absorbance at 257 nm in the darkness (solid symbols) and under UV light (opens symbols). Lines are used as a guide. Initial catalyst and PQ^{2+} concentrations were 2 g L^{-1} and 150 μM, respectively

Conclusions

It is clear that soil components such as mineral particles and humic substances affect the behavior and the mobility of pesticides in the environment. However, the results shown in this work reveal that the opposite effect also occurs, i.e., the pesticides can affect the mobility of soil constituents, as it is the case of humic acids in the solid state. The experiments show that all studied pesticides interact with HA, and this interaction could affect their mobilities through surface watercourses and

aquifers. There remains, nevertheless, an important aspect that still needs to be investigated: aggregation or precipitation of humic substances could trap pesticides and other pollutants within the solid structure protecting them, for example, from degradation, as well as demonstrated by the pesticide-clay system. Under certain conditions (high pH values, low ionic strengths), the aggregates may open its structure due to the dissolution process releasing the pollutant. These processes could have a significant environmental impact, although they have not been documented in the scientific literature up to date.

The obtained results also show that the presence of humic acid enhances the adsorption of paraquat on goethite. This could favor the deactivation of the pesticide in soils with low clay content and decrease its leaching through groundwater. In soils with high clay content, on the contrary, the solid could protect the adsorbed paraquat to be degraded. In this sense, the use mesoporous silica-based materials would result a very good alternative in environmental remediation. This type of material has a high surface area and pore size and it is easily functionalizable and reusable. In fact, its high adsorption capacity to certain pesticides could significantly reduce the contamination in soil and aqueous environments and its structure modification would accelerate the pesticide decomposition by the action of sunlight. UV-VIS spectroscopy results in this sense a novel, simple and fast method to detect metabolites, with a lower cost of analysis than chromatographic methods. However, much work is still needed to achieve a good understanding of the degradation mechanism using this technique as well as the detection and quantification of a pesticide (or several) in a multicomponent system.

References

AlOthman ZA, Apblett AW (2010) Synthesis and characterization of a hexagonal mesoporous silica with enhanced, thermal and hydrothermal stabilities. Appl Surf Sci 256(11):3573–3580. https://doi.org/10.1016/j.apsusc.2009.12.157

Arias-Estévez M, López-Periago E, Martínez-Carballo E, Simal-Gándara J, Mejuto JC, García-Río L (2008) The mobility and degradation of pesticides in soils and the pollution of groundwater resources. Agric Ecosyst Environ 123(4):247–260. https://doi.org/10.1016/j.agee.2007.07.011

Arroyave JM, Waiman CW, Zanini GP, Avena MJ (2016) Effect of humic acid on the adsorption/desorption behavior of glyphosate on goethite. Isotherms and kinetics. Chemosphere 145:34–41. https://doi.org/10.1016/j.chemosphere.2015.11.082

Barja BC, Dos Santos AM (2005) Aminomethylphosphonic acid and glyphosate adsorption onto goethite: a comparative study. Environ Sci Technol 39(2):585–592. https://doi.org/10.1021/es035055q

Barja BC, Herszage J, Dos Santos AM (2001) Iron(III)–phosphonate complexes. Polyhedron 20(15-16):1821–1830. https://doi.org/10.1016/S0277-5387(01)00741-0

Bia G, Ortiz PI, Pfaffen V, Borgnino L (2017) Humic ccid–Fe(hydr)oxide composites supported on montmorillonite: synthesis, characterization, and atrazine adsorption. J Chem Eng Data 62(11):3793–3801. https://doi.org/10.1021/acs.jced.7b00504

Brigante M, Avena M (2014) Synthesis, characterization and application of a hexagonal mesoporous silica for pesticide removal from aqueous solution. Micropor Mesopor Mat 191:1–9. https://doi.org/10.1016/j.micromeso.2014.02.035

Brigante M, Schulz PC (2011) Remotion of the antibiotic tetracycline by titania and titania–silica composed materials. J Hazard Mater 192(3):1597–1608. https://doi.org/10.1016/j.jhazmat.2011.06.082

Brigante M, Zanini G, Avena M (2013) Effects of montmorillonite on the chemical degradation kinetics of metsulfuron methyl in aqueous media. Appl Clay Sci 80-81:211–218. https://doi.org/10.1016/j.clay.2013.03.018

Brigante M, Zanini G, Avena M (2009) Effect of pH, anions and cations on the dissolution kinetics of humic acid particles. Colloid Surface A 347(1-3):180–186. https://doi.org/10.1016/j.colsurfa.2009.04.003

Brigante M, Zanini G, Avena M (2008) On the dissolution kinetics of humic acid particles. Effect of monocarboxylic acids. Chemosphere 71(11):2076–2081. https://doi.org/10.1016/j.chemosphere.2008.01.038

Brigante M, Zanini G, Avena M (2007) On the dissolution kinetics of humic acid particles. Effects of pH, temperature and Ca^{2+} concentration. Colloid Surface A 294(1-3):64–70. https://doi.org/10.1016/j.colsurfa.2006.07.045

CASAFE (2012). Mercado Argentino de Productos Fitosanitarios (Argentine Market of Plant Protection Products)/Year 2011 vs 2012. http://www.casafe.org/biblioteca/estadisticas/

Chen F, Shi R, Xue Y, Chen L, Wan QH (2010) Templated synthesis of monodisperse mesoporous maghemite/silica microspheres for magnetic separation of genomic DNA. J Magn Magn Mater 322(16):2439–2445. https://doi.org/10.1016/j.jmmm.2010.02.053

Clausen L, Fabricius I (2001) Atrazine, isoproturon, mecoprop, 2,4-D, and bentazone adsorption onto iron oxides. J Environ Qual 30(3):858–869. https://doi.org/10.2134/jeq2001.303858x

Damonte M, Sanchez R, Afonso MD (2007) Some aspects of the glyphosate adsorption on montmorillonite and its calcined form. App Clay Sci 36(1-3):86–94. https://doi.org/10.1016/j.clay.2006.04.015

Diaz Kirmser EM, Mártire DO, Gonzalez MC, Rosso JA (2010) Degradation of the herbicides clomazone, paraquat, and glyphosate by thermally activated peroxydisulfate. J Agric Food Chem 58(24):12858–12862. https://doi.org/10.1021/jf103054h

Draoui K, Denoyel R, Chgoura M, Rouquerol J (1999) Adsorption of paraquat on minerals. A thermodynamic study. J Therm Ana Calorim 58(3):597–606. https://doi.org/10.1023/A:1010152411288

Dutta A, Mandal A, Manna S, Singh SB, Berns AE, Singh N (2015) Effect of organic carbon chemistry on sorption of atrazine and metsulfuron-methyl as determined by ^{13}C-NMR and IR spectroscopy. Environ Monit Assess 187(10):620. https://doi.org/10.1007/s10661-015-4837-3

Eisenstein M (2015) Pesticides: seeking answers amid a toxic debate. Nature 521(7552):S52–S55. https://doi.org/10.1038/521S52a

Fenner K, Canonica S, Wackett LP, Elsner M (2013) Evaluating pesticide degradation in the environment: blind spots and emerging opportunities. Science 341(6147):752–758. https://doi.org/10.1126/science.1236281

Florêncio MH, Pires E, Castro AL, Nunes MR, Borges C, Costa FM (2004) Photodegradation of diquat and paraquat in aqueous solutions by titanium dioxide: evolution of degradation reactions and

characterization of intermediates. Chemosphere 55(3):345–355. https://doi.org/10.1016/j.chemosphere.2003.11.013

Fryxell GE, Mattigod SV, Lin Y, Wu H, Fiskum S, Parker K, Zheng F, Yantasee W, Zemanian TS, Shane Addleman R, Liu J, Kemner K, Kelly S, Feng X (2007) Design and synthesis of self-assembled monolayers on mesoporous supports (SAMMS): the importance of ligand posture in functional nanomaterials. J Mater Chem 17(28): 2863–2874. https://doi.org/10.1039/b702422c

Gamble DS, Bruccoleri AG (2016) Pesticide regulations for agriculture: chemically flawed regulatory practice. J Environ Sci Health B 51(8): 571–577. https://doi.org/10.1080/03601234.2016.1171646

Gautam A, Kshirsagar A, Biswas R, Banerjee S, Khanna PK (2016) Photodegradation of organic dyes based on anatase and rutile TiO_2 nanoparticles. RSC Adv 6(4):2746–2759. https://doi.org/10.1039/C5RA20861K

Goyne KW, Chorover J, Zimmerman AR, Komarneni S, Brantley SL (2004) Influence of mesoporosity on the sorption of 2,4-dichlorophenoxyacetic acid onto alumina and silica. J Colloid Interface Sci 272(1):10–20. https://doi.org/10.1016/j.jcis.2003.12.040

Hermosin MC, Cornejo J (1992) Removing 2,4-D from water by organo-clays. Chemosphere 24(10):1493–1503. https://doi.org/10.1016/0045-6535(92)90270-2

Hseu ZY, Jien SH, Cheng SF (2003) Sorption of paraquat on clay components in a Taiwan's oxisol. J Environ Sci Health B 38(4):441–449. https://doi.org/10.1081/PFC-120021664

Iglesias A, López R, Gondar D, Antelo J, Fiol S, Arce F (2010) Adsorption of paraquat on goethite and humic acid-coated goethite. J Hazard Mater 183(1-3):664–668. https://doi.org/10.1016/j.jhazmat.2010.07.077

Jankowski JJ, Kieber DJ, Mopper K (1999) Nitrate and nitrite ultraviolet actinometers. Photochem Photobiol 70(3):319–328. https://doi.org/10.1111/j.1751-1097.1999.tb08143.x

Kaur S, Kumar V, Chawla M, Cavallo L, Poater A, Upadhyay N (2017) Pesticides curbing soil fertility: effect of complexation of free metal ions. Front Chem 5:43. https://doi.org/10.3389/fchem.2017.00043

Kreunetr S, Wanchanthuek R (2017) Studies on preparation and characterization of Fe/TiO_2 catalyst in photocatalysis applications. Mater Res Express 4:076507

Kumar V, Kumar V, Upadhyay N, Sharma S (2015) Interactions of atrazine with transition metal ions in aqueous media: experimental and computational approach. 3. Biotech 5:791–798

Larrivee EM, Elkins KM, Andrews SE, Nelson DJ (2003) Fluorescence characterization of the interaction of Al^{3+} and Pd^{2+} with Suwannee River fulvic acid in the absence and presence of the herbicide 2,4-dichlorophenoxyacetic acid. J Inorg Biochem 97(1):32–45. https://doi.org/10.1016/S0162-0134(03)00239-3

Li K, Chen T, Yan L, Dai Y, Huang Z, Xiong J, Song D, Lv Y, Zeng Z (2013) Design of graphene and silica co-doped titania composites with ordered mesostructure and their simulated sunlight photocatalytic performance towards atrazine degradation. Colloid Surface A 422:90–99. https://doi.org/10.1016/j.colsurfa.2013.01.039

Liu G, Zheng S, Yin D, Xu Z, Fan J, Jiang F (2006) Adsorption of aqueous alkylphenol ethoxylate surfactants by mesoporous carbon CMK-3. J Colloid Interface Sci 302(1):47–53. https://doi.org/10.1016/j.jcis.2006.06.006

Liu W, Yang Q, Yang Z, Wang W (2016) Adsorption of 2,4-D on magnetic graphene and mechanism study. Colloid Surface A 509:367–375. https://doi.org/10.1016/j.colsurfa.2016.09.039

Mangat Echavia GR, Matzusawa F, Negishi N (2009) Photocatalytic degradation of organophosphate and phosphonoglycine pesticides using TiO_2 immobilized on silica gel. Chemosphere 76(5):595–600. https://doi.org/10.1016/j.chemosphere.2009.04.055

Milne CJ, Kinniburgh DG, Tipping E (2001) Generic NICA-Donnan model parameters for proton binding by humic substances.

Environ Sci Technol 35(10):2049–2059. https://doi.org/10.1021/es000123j

Moctezuma E, Leyva E, Monreal E, Villegas N, Infante D (1999) Photocatalytic degradation of the herbicide "Paraquat". Chemosphere 39(3):511–517. https://doi.org/10.1016/S0045-6535(98)00599-2

Nakamura T, Kawasaki N, Ogawa H, Tanada S, Kogirima M, Imaki M (1999) Adsorption removal of paraquat and diquat onto activated carbon at different adsorption temperature. Toxicol Environ 70(3-4): 275–280. https://doi.org/10.1080/02772249909358755

Nghia NM, Negishi N, Hue NT (2017) Enhanced adsorption and photocatalytic activities of co-doped TiO_2 immobilized on silica for paraquat. J Electron Mater: at press. https://doi.org/10.1007/s11664-017-5838-5

Oste LA, Van Riemsdijk WH, Temminghoff EJM (2002) Solid-solution partitioning of organic matter in soils as influenced by an increase in pH or Ca concentration. Environ Sci Technol 36(2):208–214. https://doi.org/10.1021/es0100571

Pei Z, Shan X-Q, Wen B, He B, Liu T, Xie Y, Owens G (2008) Sorption of anionic metsulfuron-methyl and cationic difenzoquat on peat and soil as affected by copper. Environ Sci Technol 42(18):6849–6854. https://doi.org/10.1021/es800807m

Phanikrishna Sharma MV, Durga Kumari V, Subrahmanyam M (2010) TiO_2 supported over porous silica photocatalysts for pesticide degradation using solar light: part 2. Silica prepared using acrylic acid emulsion. J Hazard Mater 175(1-3):1101–1105. https://doi.org/10.1016/j.jhazmat.2009.10.056

Pimentel D, Levitan L (1986) Pesticides: amounts applied and amounts reaching pests. Bioscience 36(2):86–91. https://doi.org/10.2307/1310108

Puccia V, Luengo C, Avena M (2009) Phosphate desorption kinetics from goethite as induced by arsenate. Colloid Surface A 348(1-3):221–227. https://doi.org/10.1016/j.colsurfa.2009.07.026

Ramos ME, Garcia-Palma S, Rozalen M, Johnston CT, Huertas FJ (2014) Kinetics of montmorillonite dissolution: an experimental study of the effect of oxalate. Chem Geol 363:283–292. https://doi.org/10.1016/j.chemgeo.2013.11.014

Rivoira L, Appendini M, Fiorilli S, Onida B, Del Bubba M, Bruzzoniti MC (2016) Functionalized iron oxide/SBA-15 sorbent: investigation of adsorption performance towards glyphosate herbicide. Environ Sci Pollut Res 23(21):21682–21691. https://doi.org/10.1007/s11356-016-7384-8

Roberts TR, Dyson JS, Lane MCG (2002) Deactivation of the biological activity of paraquat in the soil environment: a review of long-term environmental fate. J Agric Food Chem 50(13):3623–3631. https://doi.org/10.1021/jf011323x

Rodríguez-Cruz MS, Valderrábano M, del Hoyo C, Sánchez-Martín MJ (2009) Physicochemical study of the sorption of pesticides by wood components. J Environ Qual 38(2):719–728. https://doi.org/10.2134/jeq2008.0150

Rozalen M, Huertas FJ, Brady PV (2009) Experimental study of the effect of pH and temperature on the kinetics of montmorillonite dissolution. Geochim Cosmochim Acta 73(13):3752–3766. https://doi.org/10.1016/j.gca.2009.03.026

Rytwo G, Nir S, Margulies L (1996) A model for adsorption of divalent organic cations to montmorillonite. J Colloid Interface Sci 181(2): 551–556. https://doi.org/10.1006/jcis.1996.0412

Saito T, Koopal L, van Riemsdijk WH, Nagasaki S, Tanaka S (2004) Adsorption of humic acid on goethite: isotherms, charge adjustments, and potential profiles. Langmuir 20(3):689–700. https://doi.org/10.1021/la034806z

Sarmah AK, Kookana RS, Duffy MJ, Alston AM (2000) Hydrolysis of triasulfuron, metsulfuron-methyl and chlorsulfuron in alkaline soil and aqueous solutions. Pest Manag Sci 56(5):463–471. https://doi.org/10.1002/(SICI)1526-4998(200005)56:5<463::AID-PS138>3.0.CO;2-I

Sarmah A, Sabadie J (2002) Hydrolysis of sulfonylurea herbicides in soils and aqueous solutions: a review. J Agric Food Chem 50(22):6253–6265. https://doi.org/10.1021/jf025575p

Scrano L, Bufo SA, Emmelin C, Meallier P (2005) Abiotic degradation of the herbicide rimsulfuron on minerals and soil. In: Lichtfouse E, Schwarzbauer J, Robert D (eds) Environmental chemistry: green chemistry and pollutants in ecosystems. Springer, Berlin, pp 505–515. https://doi.org/10.1007/3-540-26531-7_46

Séquaris JM, Klumpp E, Vereecken H (2013) Colloidal properties and potential release of water-dispersible colloids in an agricultural soil depth profile. Geoderma 193-194:94–101. https://doi.org/10.1016/j.geoderma.2012.10.014

Sidhu PS, Gilkes RJ, Cornell RM, Posner AM, Quirk JP (1981) Dissolution of iron oxides and oxyhydroxides in hydrochloric and perchloric acids. Clay Clay Miner 29(4):269–276. https://doi.org/10.1346/CCMN.1981.0290404

Tanev PT, Pinnavaia TJ (1995) A neutral templating route to mesoporous molecular sieves. Science 267(5199):865–867. https://doi.org/10.1126/science.267.5199.865

Tennakone K, Kottegoda IRM (1996) Photocatalytic mineralization of paraquat dissolved in water by TiO$_2$ supported on polythene and polypropylene films. J Photochem Photobiol A 93(1):79–81. https://doi.org/10.1016/1010-6030(95)04141-9

Trivedi MK, Branton A, Trivedi D, Nayak G, Bairwa K, Jana S (2015) Spectroscopic characterization of disulfiram and nicotinic acid after biofield treatment. J Anal Bioanal Tech 6:5

Tsai WT, Hsien KJ, Chang YM, Lo CC (2005) Removal of herbicide paraquat from an aqueous solution by adsorption onto spent and treated diatomaceous earth. Bioresour Technol 96(6):657–663. https://doi.org/10.1016/j.biortech.2004.06.023

USDA. (2014). Pesticide Use in U.S. Agriculture: 21 Selected Crops, 1960-2008. Economic Information Bulletin, Number 124, May 2014. https://www.ers.usda.gov/webdocs/publications/eib124/46736_eib124_summary.pdf

USEPA, Office of Drinking Water (1987) Paraquat Health Advisory. August 1987. Draft

Vieno NM, Harkki H, Tuhkanen T, Kronberg L (2007) Occurrence of pharmaceuticals in river water and their elimination in a pilot-scale drinking water treatment plant. Environ Sci Technol 41(14):5077–5084. https://doi.org/10.1021/es062720x